INDEXING AND MAPPING OF PROTEINS USING A MODIFIED NONLINEAR SAMMON PROJECTION

Izydor Apostol[1*] and Wojciech Szpankowski[2]

[1]Baxter Hemoglobin Therapeutics Inc., Boulder, CO 80301,

[2]Purdue University, Department of Computer Science, West Lafayette, IN 47907

Summary

A modified Sammon algorithm was developed to display a relationship between proteins based on their amino acid composition. In the first stage of the method, a 19-dimensional compositional space of representative proteins was mapped into a 2-dimensional space (2-D) using the original Sammon projection creating a contour map. In the second stage, this contour map was used as a reference for new proteins projected into 2-D. Data analysis showed that proteins belonging to the same structural classes formed characteristic and distinct clusters, which could be potentially useful in the prediction of protein structural classes. However, we observed significant overlapping of the clusters which may explain the limited success of previous protein folding prediction based solely on amino acid composition. Regardless, the modified Sammon projections can generate a unique index for each individually projected protein related to its amino acid composition, which may be a useful tool in the exploratory classification of proteins.

Keywords: nonlinear Sammon projection, amino acid composition, protein structural classes, indexing of proteins.

* To whom correspondence should be addressed: Baxter Hemoglobin Therapeutics Inc., 2545 Central Ave. Boulder, CO 80301

Introduction

The classification of proteins and the prediction of their structural classes are important tasks in the characterization of newly discovered proteins. Unfortunately, the classification of proteins is limited only to a subset of proteins with enzymatic activities. Even for those, no general indexing has been widely accepted. Also, the prediction of protein folding classes based on primary sequence information remains a difficult task (1-9).

The comparison of more than two protein sequences is generally not a straightforward process. Aligning them and measuring similarity/dissimilarity distances requires complicated computing in multidimensional space equal to the length of the protein sequences. The comparison of proteins of different lengths creates an additional requirement of bringing them to the same multidimensional space which necessitates the introduction of complicated sequence gaps. It is far simpler to compare the amino acid composition (AAC) of proteins. In this case all proteins can be compared in the same 19-D compositional space. An individual protein can be described as a point or a vector in compositional space determined by the molar fractions of the 20 amino acids (10). By definition, the sum of the molar fractions of all components is equal to 1, therefore only 19 components are independent. By leaving out one component, the protein can still be unambiguously determined in 19-D space. Even in this reduced space, comparison of protein vectors is not easy, primarily due to the inabilty of humans to adequately visualize objects in spaces with greater than 3 dimensions. Several attempts have been made to use AAC information to predict protein folding classes (7,10-23). In most cases the compositional information has been brought into a linear format with the introduction of

various weighting factors and averaging methods. These procedures resulted in a significant reduction of information which limited its predictive potential.

In this work we are attempting to use Sammon mapping to project a 19-D compositional space of proteins into a 2-D space to observe the relationship between proteins within that newly created space. The algorithm works by projecting protein vectors from the compositional space onto a planar display such that the Euclidean distances between the projected images (points) approximates, as closely as possible, the corresponding distance in the original compositional space (24-26). Neither averaging nor introduction of correction/weighting factors is necessary in this method. The ability of this algorithm to capture the essential features of protein sequence or structure similarities was recently demonstrated by Agrafiotis (25) and Barlow & Richards (26).

RESULTS

Helix example of Sammon nonlinear projection

To explain the Sammon nonlinear projection algorithm, we start with a non-biological example to show how the algorithm preserves certain dependencies/shapes (e.g. helices) when projected from 3-D to 2-D space. Figure 1 displays the results obtained using the nonlinear Sammon algorithm to project 50 points distributed evenly along a 3-dimensional helix. The parametric equations for this helix are: $X = \cos Z$, $Y = \sin Z$, $Z = t / 2^{1/2}$. The points were distributed at one-unit intervals along the curve. To initiate the algorithm we selected 50 corresponding random points in 2-D space (Fig. 1A). Each point was assigned to represent one of the 50 points on the helix (3-D space). The application of the Sammon algorithm caused the 2-D points to organize in such a fashion

that the Euclidean distances between all pairs of points in 2-D space closely reflect their Euclidean distances on the helix in 3-D space. After 250 iterations for each point, using the steepest descent algorithm described in the methods section (MF =0.3), the projected points formed a highly organized wave shape (Fig. 1B), as described by Sammon (24). Figure 1C displays the results of an experiment in which one random point was excluded from the helix. The remaining 49 points were projected creating a gap in the projected wave shape. In the third experiment, the missing point was reintroduced. All 50 points were then projected but this time the X, Y coordinates of 49 points were fixed as in Figure 1C. That is, only the 50^{th} point was optimized, greatly simplifying the calculations. After only 50 iterations, the missing point fall back into the gap and completed the wave shape. The orientation of the waves in panel C and D (Figure 1) are different from that in panel B because the optimizations started from different randomly distributed points in 2-D space, resulting in different projections.

These experiments demonstrate that a set of vectors in 3-dimensional space can be projected into 2 dimensional space, recreating the dependencies from a higher dimension even if one element of the set is missing. The missing element can then be added back to the pre-computed set to complete the structure without the need to re-optimize the entire set de novo. This approach represents a significant advantage over traditional approaches because a full re-optimization "costs" n^2 versus n computations for one point optimization into the constant contour map. (*We can now extrapolate this idea to compsitional space of proteins.*)

The Sammon projection of proteins belonging to definite structure classes.

The AAC of 64 proteins classified by Chou (13) to specific structural classes were used to calculate the mole fractions of all 20 amino acids. Each protein was described as a unique vector in compositional space with coordinate factors in the range of 0 to 1 which corresponds to the molar fraction for each particular amino acid. We numbered the 64 proteins as 1,2,3…,64 according to the order listed in table 5-8 of Chou (13) or tables 2-5 of Zhang and Chou (14). All 64 protein vectors in the 19-D composition space were then projected into a 2-D space using the Sammon nonlinear algorithm. The error of the Sammon projection (Material and Methods section, eq. 1) plotted against the number of iterations using the steepest descent optimization (MF = 0.3) is shown in Figure 2. A significant degree of optimization of this projection was seen after about 75 iterations, but occasionally a burst of error was generated during later iterations. Typically, the results were analyzed following 250 iterations, well after the errors were resolved. Several projections of Chou's proteins have been made starting from different random distributions of points. In all cases the results were similar, differing primarily in the axial orientation of the projection and slightly in the resulting error. The best projection, obtained in these experiments based on the smallest Sammon's error (0.0746) is presented in Figure 3. The four different symbols correspond to four different structural classes: open squares (1-19) - 19 α proteins; open circles (20-34) - 15 β proteins; filled squares (35-48) - 14 α+β proteins; filled circles (49-64) - 16 α/β proteins. It is apparent that the structural classes formed recognizable groupings. However, a few points are clear outliers and are located outside the expected clusteres. In general, points which were "misplaced" correspond to the proteins which were also mis-assigned by the Zhang and Chou prediction algorithm (14). For example, point 32 (outside of any cluster)

corresponds to Rubredoxin which was clasified as β protein. Its unusual position can be explained by its low level of β structure (25%), lower then any other protein found in that set. The Zhang and Chou algorithm predicts α/β structural class for Rubredoxin. Point 38, which represents a High-potential Iron Protein from the α+β class, falls into the cluster of α proteins in our projection. In this case only 27 % of the total protein has a defined structure. Zhang and Chou placed this protein in the α structural class. Similar arguments could be made for other outlying points: 23, 33, 46 and 62. This may suggest that the presence of irregular protein structure can significantly influence the AAC and may result in inaccurate class assignment/prediction.

The relationship within each set of proteins was analyzed by complete-linkage cluster analysis. Cluster analysis can provide an objective automated way to group objects into clusters in multidimensional spaces. The correlation coefficient of each cluster corresponds to the maximum distance in which two objects are still considered to have similar properties. We defined the correlation coefficient as the median 2-D Euclidean distance for the set after excluding outliers (points: 23, 32, 33, 38, 46 and 62). The results of the cluster analysis are presented as outlines surrounding each set in Figure 3.

In the process of data analysis we realized that the set of 64 Chou's proteins could be too small to make a generalization about all proteins. Therefore, we examined another set of 193 proteins which has been used by Chou (19) in his latest predictions of structural classes utilizing Mahalanobis distances. This includes 129 proteins from a learning set and 64 proteins from a testing set. Proteins in both sets were selected using more precise constraints of classification (19). Compositional space of all 193 proteins was then projected into 2-D space using the nominal Sammon nonlinear algorithm. The

projection was terminated after 500 iterations (MF=0.3), and the result is shown in Figure 4. We used the same symbols as in Figure 3 to designate folding classes: open squares - 39 α proteins; open circles - 52 β proteins; filled squares - 54 α+β proteins; filled circles - 39 α/β proteins; crosses - 9 ζ (irregular) proteins. This result was not significantly different from the previously described projection of 64 proteins. As seen previously, the different structural classes formed distinct clusters in 2-D space. The α and β clusters were well separated. The α/β and α+β proteins formed smooth transitions between the α and β clusters resulting in partial overlapping of structural clusters. Irregular proteins were projected outside of the β class. As before, several points were clear outliers and were not located within their expected clusters.

Very similar results were obtained for a different set of 202 proteins. These proteins were arbitrarily selected from SCOP data base available on the World Wide Web (http://www/pdb.bnl.gov.scop) (27). Agin, the four structural classes formed distinct but overlapping clusters in 2-D space (data not shown).

These results support the early hypothesis that the folding of proteins is determined by their AAC (7,10-17,19,21). However, we observed a significant degree of overlapping between clusters (especially for β and α+β) which may explain the inaccuracy of previous protein folding prediction based solely on AAC. The irregular portions found in all proteins, may contribute significantly to the overall ambiguity.

The Sammon projection using modified distances or a reduced alphabet of amino acids.

In hope of improving clustering of structural classes, we explored several different ways of defining distance between proteins in compositional space. We examine Minkowski's l^r distance $D^*_{pq} = \left[\sum_{i=1}^{20} \left(P_i - Q_i \right)^r \right]^{\frac{1}{r}}$ for *r* ranging from 0.5 to 64 (see Material and Methods). Actually, Euclidean distance used in all the other experiments is a special case of Minkowski's definition with *r*=2. Figure 5A and 5B show the examples of the Sammon projection for *r* equal to 1 and 16 respectively. No significant differences were found in the distribution or separation of structural classes. In fact, with increased value of *r* the projected map resulted in grater overlapping of structural clusters. These data indicate that the application of Minkowski's general distance definitions does not offer any advantage over the intuitive Euclidean distance definition.

Additionally, we examined the modification of Euclidean distance by using weighting factors introduced by Chun-Ting *et al.* (17). In this particular case the calculation of Euclidean distance was modified as follows:

$$D^*_{pq} = \sqrt{\sum_{i=1}^{20} w_i \left(P_i - Q_i \right)^2}$$

The distances in compositional space were calculated as the product of w_i, the weighting factor and the Euclidean distance for each amino acid. Chun-Ting *et al.* (17) performed predictions of the structural class of proteins from AAC based on a linear-programming approach using these weighting factors. We sought to determine whether weighting factors would affect nonlinear projections. The results (Fig. 5C) indicated that these

weighting factors did not improve clustering of the proteins belonging to the same structural class.

Landes and Risler reported the successful use of a reduced amino acid alphabet in searching protein data bases (18). They reduced the 20 amino acids alphabet to 10 symbols: (A=T=S), C, (D=E=N), (F=Y), G, H, (I=L=M=V),(K=Q=R), P, W. We were interested to see if the reduction of the original compositional space into a 9-dimensional space would affect the clustering of the projected proteins. The application of the reduced alphabet into the Sammon projection of 193 proteins resulted in an irregular distribution of points (Fig. 5D). Clusters were still evident, but were not as clearly separated as in the case of the nominal projection from 19-D compositional space (Fig. 4).

Projection of proteins with unusual amino acid composition.

We investigated whetrer Sammon's projection could be used to predict the folding class of "unknown" proteins. Several hundred random proteins from the Pir1 protein data base were projected individually into the developed map shown in Figure 4. In this modified projection method, the coordinates of the 193 representative proteins which formed the contour map were held constant while the coordinates of new proteins were optimized by the Sammon algorithm. Each newly projected protein was treated as the 194^{th} element. Several projected proteins were found outside the area occupied by the four clusters of the representative set. Most of these proteins appeared to be small and/or showed unusual amino acid composition. Several of these proteins were described as unusual by Cornish-Bowden in his work on dependencies between the size and AAC of proteins (28). Additionally, we observed that if each individual protein was projected

several times, the results of the optimizations were significantly different. We believe that this was due to a lack of reference points outside the area occupied by the set of 193 representative proteins. To overcome that ambiguity, a subset of 27 extra proteins with unusual AAC were selected from the Pir1 protein data base and added to the representative set. These proteins or peptides were arbitrarily selected if their length exceeded 10 amino acids and their X, Y indices fell outside the original clusters. Adding unusual proteins expanded the representative set from 193 to 220. The expanded set was then projected using the original Sammon algorithm, forming a new expanded contour map (Fig. 6). More than 2000 proteins of randomly selected from Pir1 was then projected into the new extended contour map using the modified Sammon mapping procedure. This time we observed significantly less variability from multiple projections of the same proteins. Each protein gave a distinct point in the 2-D map. Thus, it appeared that each newly projected protein could be characterized by unique X,Y coordinates on a 2-D map, reflecting its unique amino acid composition. This method could offer a new way to classify proteins based solely on AAC.

Projection of amino acid composition of hemoglobins into the extended contour map.

The amino acid composition of porcine hemoglobin alpha chain was projected into the extended contour map as an additional 221^{th} protein. As previously described, the X,Y coordinates of the 220 proteins from the extended contour map were held as fixed points. The projected porcine hemoglobin fell into the cluster of the α proteins, close to the other hemoglobins used in the representative set. The observed index for the α chain

of the porcine hemoglobin was 0.390 ;0.630 which is very close to the other hemoglobins used in the representative set. This operation of the projection of the 221th protein was repeated for the beta chain of porcine hemoglobin and 320 other different alpha and beta globins with similar results. All of the projected α and β chains formed a distinct well defined group inside the cluster of α proteins as expected for hemoglobins (Fig. 7). Similarly, 47 protein-tyrosine kinases and 14 serine proteinases were projected into the extended contour map. These also formed distinct groups inside the α/β and β classes respectively, as would be predicted for those protein families (Fig. 7).

Additionally, a subset of 60 proteins used by Nakashima *et al*. (10) for their folding class predictions were projected into the extended contour map (data not shown). Interestingly, almost all these proteins fell into the clusters to which they had been previously classified. Together, our results indicate that the Sammon nonlinear projection can be used to predict the structural classes of unknown proteins, although some ambiguity in the assignment remains due to the overlapping of structural class clusters.

Conclusion

The nonlinear Sammon mapping algorithm may be a useful tool to examine the complicated multidimensional systems in protein science. When applied to project 19-D compositional space of proteins, it can provide a new way of mapping and indexing. We have demonstrated that proteins with similar functionality can be mapped to the same region in 2-D space. This method may have application in the prediction of folding classes and potentially functional properties of newly sequenced proteins based on compositional indices.

Our results suggest that the prediction of protein folding based on amino acid composition may never overcome certain limitations, such as overlapping clusters. Although, different structural classes of proteins form distinct clusters when projected into 2-D space, these clusters have a tendency to overlap. This overlapping of clusters may result in the ambiguous assignment of structural classes of unknown proteins, especially proteins sharing significant contributions of irregular fold. The validity of this approach depends very strongly on whether the examined set of proteins has a broad enough distribution of AAC. Therefore, it is possible that further expansion of the representative/learning set with detailed verification of the protein folds may limit overlapping and improve prediction accuracy.

We would like to point out the computational advantage of the contour map. The original Sammon algorithm (24), and its application to the protein classification as proposed by Agrafiotis (25), required N^2 computations per iteration of the steepest decent algorithm (as discussed in the Method section), where N is the number of projected proteins. In our modified method, representative proteins have been projected onto a precomputed contour map (in our experiments N=220), and new proteins were added by comparing them only individually to these N points. Therefore, the projection of compositional space for a new protein costs only 'N' computations per iteration. This difference translates to a significant saving in computation time especially for large sets of proteins.

Material and Methods

Calculation of distances between proteins in the composition space.

In the first experiment presented in Figure 1 we used the standard Euclidean distance between two points in 3-D space. The distance between two proteins (level of dissimilarity) was computed based on the amino acid composition, according to the Minkowski l^r distance (21) in equation 1:

$$D^*_{pq} = \left[\sum_{i=1}^{20} \left(P_i - Q_i \right)^r \right]^{\frac{1}{r}} \qquad (1),$$

where P_i , Q_i are the mole fraction of the i^{th} kind of amino acid in the proteins P and Q, respectively. Each protein corresponds to a point with coordinates given by the mole fraction of the 20 constituent amino acids. Except where noted, the Minkowski distance was simplified to Euclidean distance with $r=2$.

The Sammon projection

The projection of 19-D compositional space onto the 2-D Euclidean space was obtained according to the original Sammon nonlinear projection algorithm (24-26). This algorithm attempts to approximate in the best possible way (i.e., in the square error sense) a relationship between points in a multidimensional space when projected into 2-D spaces. A detail description of the algorithm has been presented by Sammon (24), so we only illustrate its meaning using a simple example. As shown below, the distance relationship in a higher dimension cannot be fully preserved in a lower dimensional space. For example, imagine three points A, B and C in 3-D space with given distances between them, defined as D^*_{AB}, D^*_{AC} and D^*_{BC}. These distances cannot be preserved in the projected 2-D space (D_{AB}, D_{AC} and D_{BC}). The best you can do is to preserve the

distance between points A and B and minimize the error (E_{AC} and E_{BC}) when locating point C.

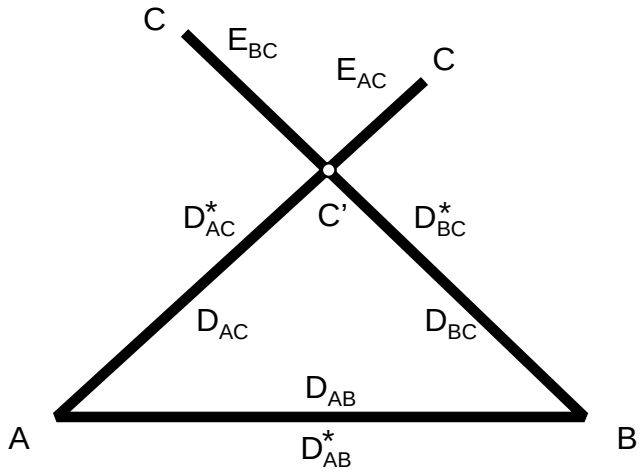

In general, the goal of Sammon's algorithm is to minimize the discrepancy in "distance" which was defined as the error of the projection:

$$E(x,y) = \frac{1}{c}\sum_{i<j}^{n} \frac{\left(D_{ij}^{*} - D_{ij}(x,y)\right)^{b}}{D_{ij}^{*}} \qquad (2)$$

where D_{ij}^{*} is a distance in original space (19-D compositional space) computed according to equation 1, $D_{ij}(x,y) = \sqrt{\left(x_i - x_j\right)^2 + \left(y_i - y_j\right)^2}$ is the Euclidean distance in 2-D space, b is a parameter, c is constant and n is the number of proteins in the representative set. It should be pointed out that the parameter b can model a variety of situations (29).

Throughout the computation, as in Agrafiotis (25), we have assumed that b=2 and

$c = \sum_{i<j}^{n} D_{ij}^{*}$.

To find optimal coordinates of a point (x, y), a numerical optimization procedure called the steepest descent algorithm was applied. In this method, the optimal solution was found in several iteration starting from a (random) initial point. In each iteration we moved towards the gradient of the function E(x,y). In the m^{th} iteration we computed the m^{th} estimate of *E(x,y)*, written as $E_{(x,y)}^{(m)}$. In the next iteration new coordinates of each point $x^{(m+1)}$, $y^{(m+1)}$ were computed according to the following formula:

for *m=1* **to** *number of iterations*

for *i=1* **to** *n*

$$x_i^{(m+1)} = x_i^{(m)} - MF \frac{\left| \frac{\partial E_{(x,y)}^{(m)}}{\partial x} \right|}{\left| \frac{\partial^2 E_{(x,y)}^{(m)}}{\partial x^2} \right|}$$

$$y_i^{(m+1)} = y_i^{(m)} - MF \frac{\left| \frac{\partial E_{(x,y)}^{(m)}}{\partial y} \right|}{\left| \frac{\partial^2 E_{(x,y)}^{(m)}}{\partial y^2} \right|}$$

end

end.

where MF ("magic factor") is an experimentally determined coefficient. The first and the second derivative of *E(x,y)* with respect to x are shown below (in a similar manner, one can compute the derivatives with respect to y):

$$\frac{\partial E_{(x,y)}^{(m)}}{\partial x} = \frac{-2}{c}\sum_{\substack{i=1 \\ i\neq j}}^{n} \frac{\left(D_{ij}^{*} - D_{ij}(x,y)\right)}{D_{ij}^{*} D_{ij}(x,y)}\left(x_i - x_j\right) \qquad (3)$$

$$\frac{\partial^2 E_{(x,y)}^{(m)}}{\partial x^2} = \frac{-2}{c}\sum_{\substack{i=1 \\ i\neq j}}^{n} \frac{1}{D_{ij}^{*} D_{ij}(x,y)}\left[\left(D_{ij}^{*} - D_{ij}(x,y)\right) - \frac{\left(x_i - x_j\right)^2}{D_{ij}(x,y)}\left(1 + \frac{D_{ij}^{*} - D_{ij}(x,y)}{D_{ij}(x,y)}\right)\right] \qquad (4)$$

In the implementation of the steepest descent method we stopped the iteration procedure after 250 cycles.

In the experiments, when additional protein *n+1* was projected into the contour map the same algorithms were used, except that the iteration procedure was used only to optimize the distance of the new protein without affecting the distances already optimized between elements of the learning set. The following modified formula was used:

for *m=1* **to** *number of iterations*

$$x_{n+1}^{(m+1)} = x_{n+1}^{(m)} - MF\frac{\left|\frac{\partial E_{(x,y)}^{(m)}}{\partial x}\right|}{\left|\frac{\partial^2 E_{(x,y)}^{(m)}}{\partial x^2}\right|}$$

$$y_{n+1}^{(m+1)} = y_{n+1}^{(m)} - MF\frac{\left|\frac{\partial E_{(x,y)}^{(m)}}{\partial y}\right|}{\left|\frac{\partial^2 E_{(x,y)}^{(m)}}{\partial y^2}\right|}$$

end.

In addition the summation of error $E_{(x,y)}$ (eq. 1) is over the single index *i* (this is only in terms of the sum).

Computer programs and data files.

The source code of the computer programs were written in Borland Turbo Pascal® version 7. Executable Windows® versions of programs (Helix.exe and SammProj.exe) used in this paper and corresponding contour maps, lists of proteins and their indices are available at http://www.cs.purdue.edu/people/spa/.

Acknowledgments

We express our special thanks to Marcin Apostol for many insightful suggestions during writing source code of computer programs. We also thank our colleagues Dr. Spencer Anthony-Cahill, Dr. Jeff Etter, Dr. Greg Flynn, Dr. Doug Lemon, Dr. Michael Weickert and the anonymous reviewers for critical reviews and helpful discussions.

References:

1. Mayoraz, E.; Dubchak, I.; Muchnik, I. Ismb 1995, 3, 240-248.

2. Muskal, S. M.; Kim, S. H. J Mol Biol 1992, 225, 713-727.

3. Lesk, A. M.; Boswell, D. R. Bioessays 1992, 14, 407-410.

4. Tuckwell, D. S.; Humphries, M. J.; Brass, A. Comput Appl Biosci 1995, 11, 627-632.

5. Garnier, J.; Gibrat, J. F.; Robson, B. Methods Enzymol 1996, 266, 540-553.

6. Fasman, G. D. Ed. Prediction of Protein Structure and the Principles of Protein Conformation, Plenum Press, New York, 1989.

7. Jaroszewski, L.; Rychlewski, L.; Zhang, B.; Godzik, A. Protein Sci 1998, 7, 1431-1440.

8. Fischer, D.; Eisenberg, D. Protein Sci 1996, 5, 947-955.

9. Onuchic, J. N.; Luthey-Schulten, Z.; Wolynes, P. G. Annu Rev Phys Chem 1997, 48, 545-600.

10. Nakashima, H.; Nishikawa, K.; Ooi, T. J Biochem (Tokyo) 1986, 99, 153-162.

11. Hatch, F. T. Nature 1965, 206, 777-779.

12. Harding, J. J. Biochem J 1984, 217, 339-340.

13. Chou, P. Y. Prediction of Protein Structure and the Principles of Protein Conformation (Fasman, G. D. Ed.), pp. 549-586, Plenum Press, New York, 1989.

14. Zhang, C. T.; Chou, K. C. Protein Sci 1992, 1, 401-408.

15. Dubchak, I.; Holbrook, S. R.; Kim, S. H. Proteins 1993, 16, 79-91.

16. Nakai, K.; Kidera, A.; Kanehisa, M. Protein Eng 1988, 2, 93-100.

17. Chun-Ting, Z.; Xinhua, X.; Genfa, Z. Eur J Biochem 1992, 210, 747-749.

18. Landes, C.; Risler, J. L. Comput Appl Biosci 1994, 10, 453-454.

19. Chou, K. C. Proteins 1995, 21, 319-344.

20. Chou, K. C. FEBS Lett 1995, 363, 127-131.

21. Chou, K. C.; Zhang, C. T. Crit Rev Biochem Mol Biol 1995, 30, 275-349.

22. Chou, K. C.; Zhang, C. T. J Biol Chem 1994, 269, 22014-22020.

23. Chou, K. C.; Maggiora, G. M. Protein Eng 1998, 11, 523-538.

24. Sammon, J. W. IEEE Trans Comp 1969, C-18, 401-409.

25. Agrafiotis, D. K. Protein Sci 1997, 6, 287-293.

26. Barlow, T. W.; Richards, W. G. J Mol Graph 1995, 13, 373-376.

27. Murzin, A. G.; Brenner, S. E.; Hubbard, T.; Chothia, C. J Mol Biol 1995, 247, 536-540.

28. Cornish-Bowden, A. Biochem J 1983, 213, 271-274.

29. Szpankowski, W. SIAM J Computing 1993, 22, 1176-1198.

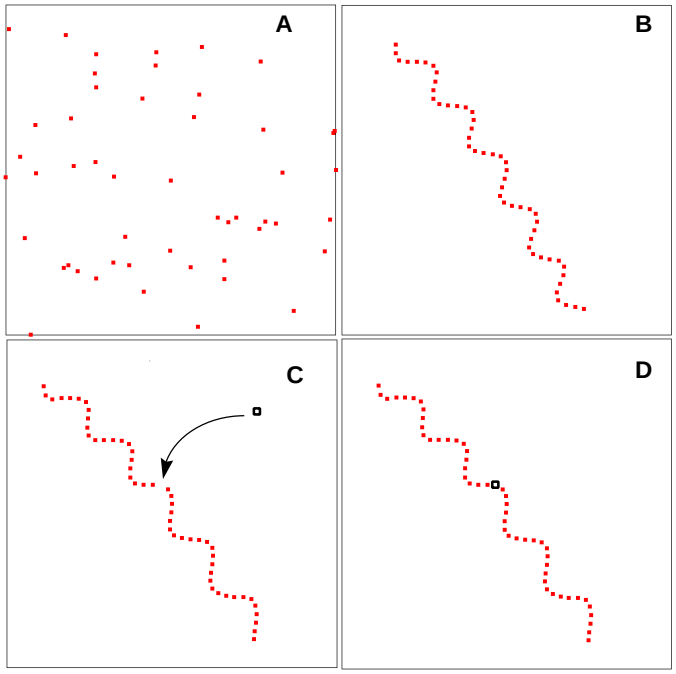

Figure 1. Sammon projection of a helix: A-starting random distribution of 50 points, B-optimized projection (map) of 50 points after 250 iterations, C-contour map of 49 points (1 selected point is missing from the map of 50 points) after 250 iterations, D-projection of the missing 50th point into the contour map after 50 further iterations.

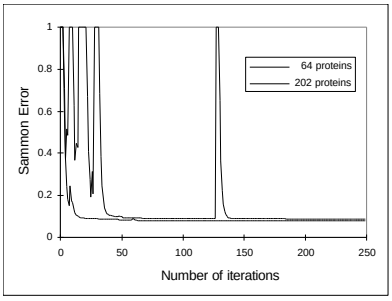

Figure 2. Error of Sammon projection (MF=0.3) plotted against number of iteration for sets of 64 (solid line) and 202 (dashed line) projected proteins.

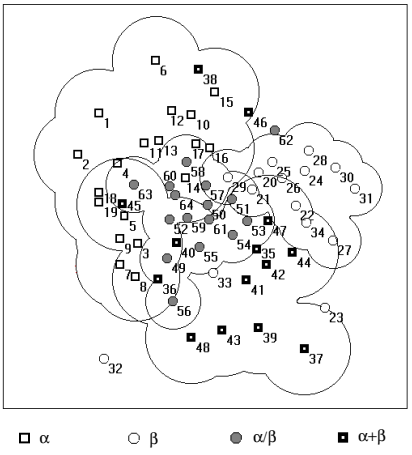

Figure 3. 2-D contour map of compositional space of Chou's 64 proteins (13) belonging to four different folding classes. Open squares - 19α proteins; open circles - 15 β proteins; filled squares - 14 a+β proteins; filed circles - 16 α/β proteins. Outlines were drawn based on cluster analysis for each structural class. Optimization was terminated after 250 iterations (MF=0.3). The error of the projection was 0.0746.

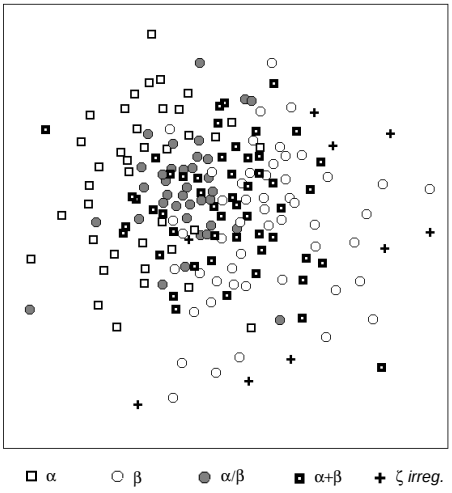

Figure 4. 2-D contour map of compositional space of Chou's 193 proteins (19) belonging to different folding classes: open squares - 39 α proteins; open circles - 52 β proteins; filled squares - 54 α+β proteins; filed circles - 39 α/β proteins; crosses - 9 ζ (irregular) proteins. Optimization was terminated after 500 iterations (MF=0.3). The error of the projection was 0.151.

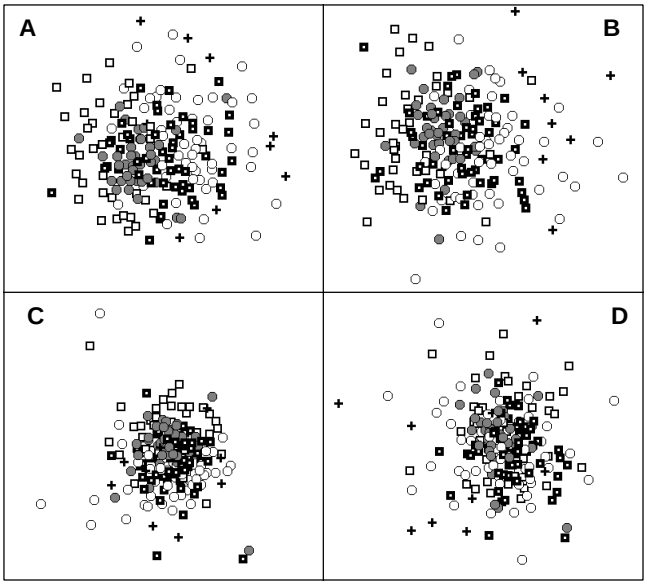

Figure 5. Sammon projection of Chou's 193 proteins (19) after 250 iterations using (MF=0.3): A - Minkowski distance for r=1, B Minkowski distance for r=16, C - Euclidean distance modified by weighting factors (17), D - a reduced amino acid alphabet (18).

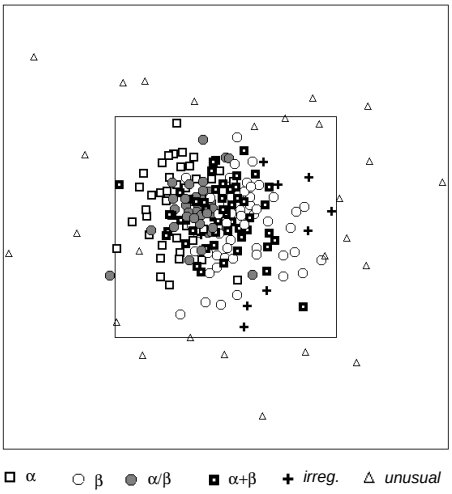

Figure 6. 2-D contour map of 220 proteins. The set of 193 proteins (Fig.3) was appended with additional 27 proteins with unusual composition (Appendix A). After 500 iteration (MF=0.3) the error of the Sammon projection was 0.135.

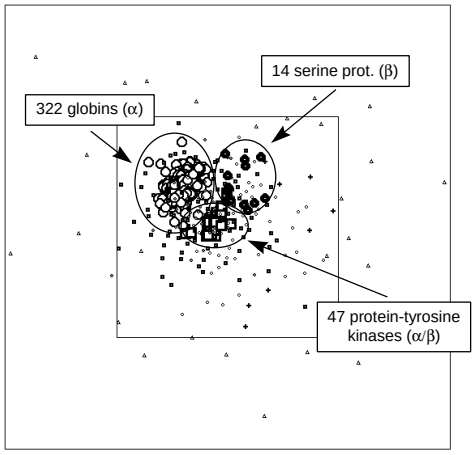

Figure 7. Projection of: 321diffrent alpha and beta hemoglobin subunits (open circles), 47 protein-tyrosine kinases (open squares), and 14 serine proteinases (filled circles) into the 220 proteins contour map. 50 rounds of optimization (MF =0.3) was performed for each added protein.

Appendix A.

Amino acid composition of the 27 unusual proteins (unusual amino acid composition). The data for each protein contain two lines: its length, Pir code and name. The second line gives the frequencies of 20 amino acids according to the alphabetical order of the sir ACDEFGHIKLMNPQRSTVWY.

```
430    P1;HHBYD8     Heat shock protein DDR48 - Yeast (Saccharomyces cerevisiae)
 0.47  0.00 13.49  0.70  1.16 11.40  0.00  0.70  6.98  0.23  0.70 23.26  0.00  1.63  1.40 26.51  0.47
109    P1;TNHUA      Prothymosin alpha - Human
10.09  0.00 17.43 31.19  0.00  8.26  0.00  0.92  7.34  0.92  0.00  5.50  0.92  1.83 1.83  3.67  5.50
75     P1;TISYD2     proteinase inhibitor (Bowman-Birk) D-II - soybean
 0.00 18.67 14.67  2.67  1.33  1.33  1.33  1.33  5.33  4.00  4.00  2.67  6.67  5.33  6.67 16.00  4.00
61     P1;FECF       Ferredoxin - Chlorobium sp.
19.67 14.75  3.28 11.48  1.64  8.20  0.00  8.20  0.00  1.64  0.00  1.64  6.56  1.64  0.00  3.28  6.56
61     P1;PIHUPF     Basic proline-rich peptide P-F - Human
 1.64  0.00  0.00  0.00  0.00 22.95  0.00  0.00  8.20  0.00  0.00  3.28 40.98 14.75  1.64  6.56  0.00
51     P1;HSBOS      Sperm histone - Bovine
 1.96 13.73  0.00  0.00  1.96  3.92  1.96  1.96  0.00  1.96  1.96  0.00  0.00  1.96 50.98  3.92  5.88
48     P1;EWBY8      H+-transporting ATP synthase
 0.00  0.00  0.00  0.00 14.58  2.08  0.00  8.33  2.08 25.00  8.33  2.08  6.25  6.25  4.17  6.25  4.17
38     P1;C32038     mu-agatoxin III - funnel-weaving spider (Agelenopsis aperta)
 7.89 21.05 10.53  0.00  0.00 10.53  0.00  0.00  0.00  0.00  2.63  0.00  5.26  2.63 10.53 13.16  0.00
14     P1;QMVHMM     mastoparan M - hornet (Vespa mandarinia)
28.57  0.00  0.00  0.00  0.00  0.00  0.00 14.29 21.43 28.57  0.00  7.14  0.00  0.00  0.00  0.00  0.00
13     P1;JTJG3      Tremerogen a-13 - Basidiomycete (Tremella mesenterica)
 0.00  7.69  7.69  7.69  0.00 38.46  0.00  0.00  0.00  0.00  0.00  7.69  7.69  0.00  7.69  7.69  0.00
11     P1;XASNBA     Bradykinin-potentiating peptide B - Mamushi
 0.00  0.00  0.00  0.00  0.00  9.09  0.00  9.09  9.09  9.09  0.00  0.00 45.45  9.09  9.09  0.00  0.00
10     P1;AKLQ             Adipokinetic hormone - Migratory locust
 0.00  0.00  0.00  0.00 10.00 10.00  0.00  0.00  0.00 10.00  0.00 20.00 10.00 10.00  0.00  0.00 20.00
10     P1;SPPGNK     neuromedin K - pig
 0.00  0.00 20.00  0.00 20.00 10.00 10.00  0.00  0.00 10.00 20.00  0.00  0.00  0.00  0.00  0.00  0.00
259    P1;TPRBTS     Troponin T, skeletal muscle - Rabbit
10.04  0.00  5.79 18.15  1.93  3.09  2.32  3.09 15.06  7.34  1.93 1.93  3.47  3.86  9.65  3.47  2.32
61     P1;SMHU1F     Metallothionein 1F - Human
 8.20 32.79  3.28  3.28  0.00  8.20  0.00  0.00 13.11  0.00  1.64  1.64  3.28  1.64  0.00 14.75  3.28
13     P1;UNBO       neurotensin - bovine
 0.00  0.00  0.00  7.69  0.00  0.00  0.00  7.69  7.69 15.38  0.00  7.69 15.38  7.69 15.38  0.00  0.00
14     P1;QMWAVV     mastoparan - yellowjacket (Vespula lewisii)
28.57  0.00  0.00  0.00  0.00  0.00  0.00 14.29 21.43 28.57  0.00  7.14  0.00  0.00  0.00  0.00  0.00
22     P1;MXKN1      mu-conotoxin GIIIA - cone shell (Conus geographus)
 4.55 27.27  9.09  0.00  0.00  0.00  0.00  0.00 18.18  0.00  0.00  0.00 13.64  9.09 13.64  0.00  4.55
82     P1;QFBO       micro glutamic acid-rich protein - bovine
18.29  0.00  4.88 47.56  0.00  8.54  0.00  0.00 12.20  0.00  0.00  0.00  2.44  2.44  0.00  1.22  2.44
```

* To whom correspondence should be addressed: Baxter Hemoglobin Therapeutics Inc., 2545 Central Ave. Boulder, CO 80301

```
40      P1;FDFI8     Antifreeze protein GS-8 - Grubby sculpin
60.00  0.00  5.00  2.50  0.00  2.50  0.00  2.50  7.50  5.00  2.50  0.00  2.50 2.50  2.50  0.00  5.00
291     P1;EEWTG     gamma-gliadin B precursor - wheat
 4.12  2.75  0.69  1.03  4.47  2.75  1.37  6.87  1.37  8.25  2.06  1.37 15.12 30.24  1.37  6.19  3.09
29      P1;SNUMP     sillucin - Rhizomucor pusillus
3.45 27.59  0.00  0.00  0.00 13.79  0.00  3.45  6.90  3.45  0.00  3.45  3.45  3.45  3.45 10.34  3.45
221     P1;KGZQH     histidine/alanine-rich protein - Plasmodium falciparum
27.60  0.45  7.24  0.90  3.17  3.62 27.15  0.45  2.71  4.98  0.45 12.67  0.00  0.45 0.45  4.52  1.36
61      P1;DNVPB     DNA-binding protein - budgerigar fledgling disease virus
9.84  0.00  0.00  0.00  0.00  1.64  1.64  0.00  1.64 34.43  1.64  3.28 14.75  6.56 14.75  6.56  3.28
44      P1;W5WLE     E5 protein - bovine papillomavirus type 1
4.55  4.55  2.27  2.27 15.91  4.55  2.27  0.00  0.00 34.09  4.55  2.27  4.55  2.27  0.00  2.27  2.27
660    P1;QQBE3     BHLF1 protein - human herpesvirus 4 (strain B95-8)
16.06  2.58  2.12  2.27  0.15 15.76  2.42  0.00  0.00  2.88  0.15  1.06 22.12  5.61 13.94  5.30  5.30
65     >P1;VHNVBM    nucleocapsid protein - Bombyx mori nuclear polyhedrosis virus
3.08  0.00  0.00  0.00  0.00  7.69  0.00  1.54  0.00  3.08  1.54  0.00  3.08  0.00 40.00 16.92 10.77
```